Hindawi Publishing Corporation
EURASIP Journal on Wireless Communications and Networking
Volume 2010, Article ID 868314, 10 pages
doi:10.1155/2010/868314

Research Article

Multicarrier Communications Based on the Affine Fourier Transform in Doubly-Dispersive Channels

Djuro Stojanović,[1] Igor Djurović,[2] and Branimir R. Vojcic[3]

[1] *Crnogorski Telekom, Podgorica 81000, Montenegro*
[2] *Electrical Engineering Department, University of Montenegro, Podgorica 81000, Montenegro*
[3] *Department of Electrical and Computer Engineering, The George Washington University, Washington, DC 20052, USA*

Correspondence should be addressed to Djuro Stojanović, djuros@t-com.me

Received 6 October 2010; Accepted 16 December 2010

Academic Editor: Pascal Chevalier

The affine Fourier transform (AFT), a general formulation of chirp transforms, has been recently proposed for use in multicarrier communications. The AFT-based multicarrier (AFT-MC) system can be considered as a generalization of the orthogonal frequency division multiplexing (OFDM), frequently used in modern wireless communications. AFT-MC keeps all important properties of OFDM and, in addition, gives a new degree of freedom in suppressing interference caused by Doppler spreading in time-varying multipath channels. We present a general interference analysis of the AFT-MC system that models both time and frequency dispersion effects. Upper and lower bounds on interference power are given, followed by interference power approximation that significantly simplifies interference analysis. The optimal parameters are obtained in the closed form followed by the analysis of the effects of synchronization errors and the optimal symbol period. A detailed interference analysis and optimal parameters are given for different aeronautical and land-mobile satellite (LMS) channel scenarios. It is shown that the AFT-MC system is able to match changes in these channels and efficiently reduce interference with high-spectral efficiency.

1. Introduction

The multicarrier system based on the affine Fourier transform (AFT-MC), a generalization of the Fourier (FT) and fractional Fourier transform (FrFT), has been recently proposed as a technique for transmission in the wireless channels [1]. The interference analysis of AFT-MC system has been presented in [2]. However, the performance of the AFT-MC system has been analyzed under the assumption that the guard interval (GI) eliminates all effects of multipath delays.

In this paper, we generalize interference analysis of AFT-MC system taking into consideration all multipath and Doppler spreading effects of doubly-dispersive channels. Upper and lower bounds on the interference in the AFT-MC system are obtained. These bounds are generalizations of results for the OFDM from [3] and for the AFT-MC with the GI from [2]. Furthermore, an approximation of the interference power is proposed, leading to a simple performance analysis. It is shown that implementation of the AFT-MC leads to a significant reduction of the total interference in the presence of large Doppler spreads, even when the GI is not used. A calculation of the optimal parameters, followed by the analysis of the effects of synchronization errors, is performed. We also present a closed form calculation of the optimal symbol period that maximizes spectral efficiency. It is shown that the spectral efficiency higher than 95% can be achievable simultaneously with significantly interference reduction.

In doubly dispersive channels, interference is composed of intersymbol interference (ISI) and intercarrier interference (ICI). The ISI is caused by the time dispersion due to the multipath propagation, whereas the ICI is caused by the frequency dispersion (Doppler spreading) due to the motion of the scatterers, transmitter, or receiver. In order to characterize the difference between time-dispersive and non-time-dispersive (frequency-flat) interference effects, analyses have been performed for the cases when the GI is not employed (time-dispersive) and when the GI is employed

(non-time-dispersive). Since AFT-MC represents a general case, these results are also generalization of interference characterization of OFDM and FrFT-MC systems.

A practical interference analysis and implementation of AFT-MC system is given for aeronautical and land-mobile satellite (LMS) systems. The conventional aeronautical communications systems use analog Amplitude Modulations (AM) technique in the Very High Frequency (VHF) band. In order to improve efficiency and safety of radio communications, it is necessary to introduce new digital transmission techniques [4]. Digital multicarrier systems have been identified as the best candidates for meeting the future aeronautical communications, primarily due to bandwidth efficiency and high robustness against interference. Although OFDM is the first choice as the most popular multicarrier modulation, its Fourier basis is not optimal for transmission in the aeronautical channels. A detail analysis of interference characterization of each of the stage of the flight (en-route, arrival and takeoff, taxi, and parking) is given. The en-route stage represents the main phase of flight and the most critical one, due to significant velocities and corresponding time-varying impairments that severely derogate the communications. In en-route scenario, the AFT-MC system transmits almost without interference, whereas in all other scenarios, it either outperforms or it has the same interference suppression characteristics as the OFDM system. This makes AFT-MC a promising candidate for future aeronautical multicarrier modulation technique. In order to exploit all potential of AFT-MC in real-life implementation, a through analysis of its properties, presented in the paper, is of the most importance.

The LMS communications with directional antennas represent another example of channels where the AFT-MC system significantly suppresses interference by exploiting channel properties. The LMS systems have found rapidly growing application in navigation, communications, and broadcasting [5]. They are identified as superior to terrestrial mobile communications in areas with small population or low infrastructure [6]. The results of our analysis show that the AFT-MC system outperforms OFDM in the LMS channels when directional antennas are used, and it represents an efficient, interference resilient, transmission system.

In summary, the mathematical model for generalized interference analysis of AFT-MC system taking into consideration all multipath and Doppler spreading effects of doubly-dispersive channels is presented, and the upper and lower bounds on the interference for the AFT-MC system are obtained. Furthermore, an approximation of the interference power that includes both time and Doppler spreading effects is given, followed by the analysis of the synchronization effects errors and calculation of optimal symbol period. A detailed interference analysis and optimal parameters are given for different aeronautical and LMS channel scenarios, showing potential of practical implementation of AFT-MC systems.

The paper is organized as follows. The signaling performance of the AFT-MC system is introduced in Section 2, followed by the optimal parameters modeling in Section 3. Practical implementation in aeronautical and LMS channels are presented in Section 4. Finally, conclusions are given in Section 5.

2. Signaling Performance

2.1. Bounds on the Interference. The baseband equivalent of the AFT-MC system signal can be expressed as

$$s(t) = \sum_{n=-\infty}^{\infty} \sum_{k=0}^{M-1} c_{n,k} g(t - nT) e^{j2\pi(c_1(t-nT)^2 + c_2 k^2 + (k/T)(t-nT))}, \tag{1}$$

where M is the total number of subcarriers, $\{c_{n,k}\}$ are data symbols, n and k are the symbol interval and subcarrier number, respectively, $g(t - nT)$ represent the translations of a single normalized pulse shape $g(t)$, T is the symbol period, and c_1 and c_2 are the AFT parameters. The data symbols are assumed to be statistically independent, identically distributed, and with zero-mean and unit-variance.

The signal at the receiver is given as [7]

$$r(t) = (\mathbf{H}s)(t) + n(t), \tag{2}$$

where multipath fading linear operator $\mathbf{H}$ models the baseband doubly dispersive channel and $n(t)$ represents the additive white Gaussian noise (AWGN), with the one-sided power spectral density N_0. Usually, the frequency offset correction block, that can be modeled as $e^{j2\pi c_0 t}$, is inserted in the receiver.

The interference power P_I in practical wireless channels, where both time and frequency spread have finite support, that is, $\tau \in [0, \tau_{\max}]$ and $\nu \in [-\nu_d, \nu_d]$, can be expressed as [2]

$$P_I = 1 - \int_{-\nu_d}^{\nu_d} \int_{0}^{\tau_{\max}} S(\tau, \nu) \left| A\left(\tau_p, \nu_p\right) \right|^2_{\substack{n=n' \\ k=k'}} d\tau \, d\nu, \tag{3}$$

where $S(\tau, \nu)$ denotes a scattering function that completely characterizes the WSSUS channel, $A(\tau_p, \nu_p)$ represents the linearly transformed ambiguity function, and τ_p, and ν_p equal

$$\begin{aligned} \tau_p &= (n' - n)T + \tau, \\ \nu_p &= \frac{1}{T}(k' - k) + \nu - c_0 - 2c_1((n' - n)T + \tau), \end{aligned} \tag{4}$$

respectively. AFT represents a general chirp-based transform and other variations such as the fractional FT (FrFT) with optimal parameters can be also implemented in channel with the same effectiveness. Results for the FrFT with order α and ordinary OFDM (the FT based system) can be easily obtained by substituting $c_1 = \cot\alpha/(4\pi)$ and $c_1 = 0$, respectively.

Time-varying multipath channels introduce effects of multipath propagation and Doppler spreading. To obtain an expression for the interference power in general case, we assume that the GI has not been inserted. Note that results of the AFT-MC interference analysis from [2], where it has been assumed that the GI eliminates effects of multipath, represent

just a special case of frequency flat channel. Now, $|A(\tau_p,\nu_p)|^2$ for $n'=n$ and $k'=k$ can be expressed as

$$\left|A\left(\tau_p,\nu_p\right)\right|^2_{\substack{n=n'\\k=k'}} = \frac{\sin^2\pi(\nu-c_0-2c_1\tau)(T-\tau)}{\pi^2(\nu-c_0-2c_1\tau)^2T^2}. \tag{5}$$

The interference power (3) can be expressed as

$$P_I = 1-\int_{-\nu_d}^{\nu_d}\int_0^{\tau_{\max}} S(\tau,\nu)\frac{\sin^2\pi(\nu-c_0-2c_1\tau)(T-\tau)}{\pi^2(\nu-c_0-2c_1\tau)^2T^2}d\tau\,d\nu. \tag{6}$$

Knowing that $\sin^2(\theta/2)=(1/2)(1-\cos\theta)$, we can calculate the upper and lower bounds on the interference by using the truncated Taylor series [8]

$$\frac{1}{2}\theta^2-\frac{1}{24}\theta^4 \le 1-\cos\theta \le \frac{1}{2}\theta^2-\frac{1}{24}\theta^4+\frac{1}{720}\theta^6. \tag{7}$$

Inserting (7) into (6), the upper and lower bounds can be expressed as

$$\begin{aligned} P_{\mathrm{IUB}} &= P_{\mathrm{ICI}}^{\mathrm{UB}}+P_{\mathrm{ISI}}^{\mathrm{UB}}+P_{\mathrm{ICSI}}^{\mathrm{UB}},\\ P_{\mathrm{ILB}} &= P_{\mathrm{ICI}}^{\mathrm{LB}}+P_{\mathrm{ISI}}^{\mathrm{LB}}+P_{\mathrm{ICSI}}^{\mathrm{LB}}, \end{aligned} \tag{8}$$

where

$$P_{\mathrm{ICI}}^{\mathrm{UB}} = \frac{1}{3}m_{20}(c_0,c_1)\pi^2T^2, \tag{9}$$

$$P_{\mathrm{ISI}}^{\mathrm{UB}} = 2m_{01}(c_0,c_1)\frac{1}{T}-m_{02}(c_0,c_1)\frac{1}{T^2}, \tag{10}$$

$$\begin{aligned} P_{\mathrm{ICSI}}^{\mathrm{UB}} &= -\frac{4}{3}m_{21}(c_0,c_1)\pi^2T+2m_{22}(c_0,c_1)\pi^2\\ &\quad -\frac{4}{3}m_{23}(c_0,c_1)\pi^2\frac{1}{T}+\frac{1}{3}m_{24}(c_0,c_1)\pi^2\frac{1}{T^2}, \end{aligned} \tag{11}$$

$$P_{\mathrm{ICI}}^{\mathrm{LB}} = P_{\mathrm{ICI}}^{\mathrm{UB}}-\frac{2}{45}m_{40}(c_0,c_1)\pi^4T^4,$$

$$P_{\mathrm{ISI}}^{\mathrm{LB}} = P_{\mathrm{ISI}}^{\mathrm{UB}},$$

$$\begin{aligned} P_{\mathrm{ICSI}}^{\mathrm{LB}} &= P_{\mathrm{ICSI}}^{\mathrm{UB}}+\frac{4}{15}m_{41}(c_0,c_1)\pi^4T^3-\frac{2}{3}m_{42}(c_0,c_1)\pi^4T^2\\ &\quad +\frac{8}{9}m_{43}(c_0,c_1)\pi^4T-\frac{2}{3}m_{44}(c_0,c_1)\pi^4\\ &\quad +\frac{4}{15}m_{45}(c_0,c_1)\pi^4\frac{1}{T}-\frac{2}{45}m_{46}(c_0,c_1)\pi^4\frac{1}{T^2}. \end{aligned} \tag{12}$$

Moments of the scattering function $m_{ij}(c_0,c_1)$ are defined as

$$m_{ij}(c_0,c_1) = \int_{-\nu_d}^{\nu_d}\int_0^{\tau_{\max}} S(\tau,\nu)(\nu-c_0-2c_1\tau)^i\tau^j d\tau\,d\nu. \tag{13}$$

The OFDM moments $m_{ij}(0,0)$ can be obtained for $c_0=0$ and $c_1=0$. The AFT-MC moments $m_{ij}(c_0,c_1)$ can be calculated from OFDM moments $m_{ij}(0,0)$ as [2]

$$\begin{aligned} m_{ij}(c_0,c_1) &= \sum_{k=0}^{i}\sum_{l=0}^{i-k}(-1)^{l+k}\binom{i}{k}\binom{i-k}{l}\\ &\quad\times c_0^l(2c_1)^k m_{i-k-l,k+j}(0,0). \end{aligned} \tag{14}$$

In a similar manner, parameters $m_{ij}(c_0,0)$ for the OFDM with the offset correction can be expressed as

$$m_{ij}(c_0,0) = \sum_{k=0}^{i}(-1)^k\binom{i}{k}c_0^k m_{i-k,j}(0,0). \tag{15}$$

2.2. Interference Approximation. Let us now analyze a Taylor expansion approximation error. Since the Taylor expansion is an infinite series, there will be always omitted terms. Therefore, the Taylor series in (7) accurately represents $\cos\theta$ only for $\theta \ll 1$. In the OFDM system, $\theta \ll 1$ can be expressed as $\nu_d T \ll 1$. This restriction can be interpreted as the request that time-varying effects in the channel are sufficiently slow, and symbol duration is always smaller than the coherence time, what is typically satisfied in practical mobile radio fading channels [9] access technology. Symbol duration in IEEE 802.16 (ETSI, 3.5 MHz bandwidth mode) is $T=64\,\mu$s and the GI $T_{\mathrm{CP}}=2,4,8,16\,\mu$s, whereas in LTE architecture $T=66.7\,\mu$s and $T_{\mathrm{CP}}=4.7\,\mu$s. For these system parameters, $\nu_d T \ll 1$, for approximately $\nu_d \ll 10^4$ Hz. In land mobile communications, this assumption is satisfied, since Doppler shifts larger than 10^3 Hz do not usually occur. However, in aeronautical and satellite communications, $\nu_d T \ll 1$ is not always satisfied since Doppler shifts larger than 10^3 Hz may occur due to high velocity of the objects. A simple solution of reducing T accordingly to keep the product low cannot be implemented since T becomes close to or even smaller than the multipath delays.

In the AFT-MC system, $\theta \ll 1$ can be expressed as $(\nu_d+|c_0|+2|c_1|\tau_{\max})T \ll 1$, and bounds stay close to the exact result for approximately $(\nu_d+|c_0|+2|c_1|\tau_{\max})T<0.25$. Actually, the upper and lower bounds are so close that they are practically indistinguishable. However, for $(\nu_d+|c_0|+2|c_1|\tau_{\max})T>1$ (e.g., symbol interval and velocity are large) the interference bounds diverge toward infinity, whereas the exact interference power converges towards the power of diffused components $1/(K+1)$, where K denotes the Rician factor.

Therefore, in order to accurately approximate the interference power, these constrains should be taken into consideration. An approximation of the interference power for the wide range of channel parameters including $(\nu_d+|c_0|+2|c_1|\tau_{\max})T>1$ can be made by modification of the upper bound as

$$P_I \cong P_{\mathrm{ISI}}^{\mathrm{UB}}+\frac{\left(1/(K+1)-P_{\mathrm{ISI}}^{\mathrm{UB}}\right)\left(P_{\mathrm{ICI}}^{\mathrm{UB}}+P_{\mathrm{ICSI}}^{\mathrm{UB}}\right)}{1/(K+1)-P_{\mathrm{ISI}}^{\mathrm{UB}}+P_{\mathrm{ICI}}^{\mathrm{UB}}+P_{\mathrm{ICSI}}^{\mathrm{UB}}}, \tag{16}$$

where $P_{\mathrm{ISI}}^{\mathrm{UB}}$, $P_{\mathrm{ICI}}^{\mathrm{UB}}$, and $P_{\mathrm{ICSI}}^{\mathrm{UB}}$ are defined in (9), (10), and (11), respectively.

Figure 1 shows the comparison of upper and lower bounds, approximation and exact interference power for the AFT-MC system without the GI. The channel is modeled by classical Jakes Doppler Power Profile (DPP) and rural area (RA) multipath line-of sight (LOS) environment with an exponential Power Delay Profile (PDP) as defined in COST 207 [10]. The AFT-MC and channel parameters are $c_0=356$ Hz, $c_1=-8.5\cdot10^8$ Hz^2, $\nu_d=517$ Hz, $\nu_{\mathrm{LOS}}=0.7\nu_d$, $K=15$ dB, $\tau_{\max}=0.7\,\mu$s, and $T\in[10\,\mu\mathrm{s},2\,\mathrm{ms}]$. From Figure 1,

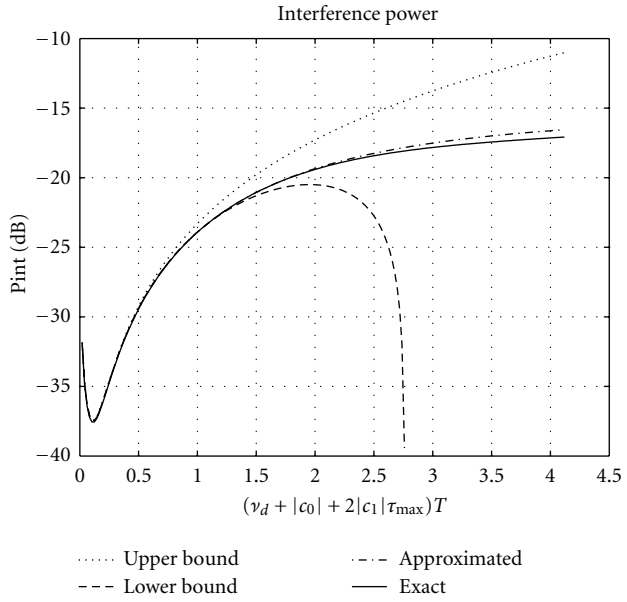

Figure 1: Comparison of the upper and lower bound, approximated and exact interference power for the AFT-MC system without the GI.

it can be seen that the upper and lower bounds are close only for $(\nu_d + |c_0| + 2|c_1|\tau_{\max})T < 0.25$, whereas the approximated interference power stays close to the exact interference power in the whole range (difference is around 1 dB, when $(\nu_d + |c_0| + 2|c_1|\tau_{\max})T > 1$).

Note that if sufficient GI is inserted, effects of multipath delays are eliminated and the approximation of interference power simplifies to [2]

$$P_I \cong \frac{(1/(K+1))P_{\text{ICI}}^{\text{UB}}}{1/(K+1) + P_{\text{ICI}}^{\text{UB}}}. \tag{17}$$

3. Optimal Parameters

3.1. Channel Models. Multipath scenario with LOS component represents a general channel model in aeronautical and LMS communications. We assume that the LOS component with power $K/(K+1)$ arrives at $\tau = 0$ with frequency offset ν_{LOS}. Multipath components are modeled by the scattering function $S_{\text{diff}}(\tau, \nu)$ with power $1/(K+1)$.

A general scattering function can be defined as

$$S(\tau, \nu) = \frac{K}{K+1}\delta(\tau)\delta(\nu - \nu_{\text{LOS}}) + \frac{1}{K+1}S_{\text{diff}}(\tau, \nu). \tag{18}$$

Analysis of channel behavior depends on the $S_{\text{diff}}(\tau, \nu)$ properties. There are three characteristic cases:

(1) multipath scenario with LOS component and separable scattering function,

(2) multipath scenario with LOS component and cluster of scattered paths,

(3) multipath scenario with two-paths.

For each of special cases, the optimal parameters for the AFT-MC system and interference power can be calculated in the closed form.

Optimal parameters $c_{0\text{opt}}$ and $c_{1\text{opt}}$ can be obtained as [11]

$$\begin{aligned} c_{0\text{opt}} &= \frac{m_{02}(0,0)m_{10}(0,0) - m_{01}(0,0)m_{11}(0,0)}{m_{02}(0,0) - m_{01}^2(0,0)}, \\ c_{1\text{opt}} &= \frac{m_{11}(0,0) - m_{01}(0,0)m_{10}(0,0)}{2\left(m_{02}(0,0) - m_{01}^2(0,0)\right)}. \end{aligned} \tag{19}$$

Moments $m_{20}(0,0)$ and $m_{02}(0,0)$ represent the Doppler spread ν_m and delay spread τ_m of the channel in the OFDM system, respectively. Moments $m_{10}(0,0)$ and $m_{01}(0,0)$ quantify the average Doppler shift ν_e and delay shift τ_e, respectively. In typical wireless scenario, the scattering function $S(\tau, \nu)$ can be decomposed via the PDP $Q(\tau)$ and DPP $P(\nu)$ and $m_{11}(0,0)$ can be calculated using $m_{01}(0,0)$ and $m_{10}(0,0)$. Thus, the AFT parameters in real-life environment can be calculated using estimations of the Doppler and delay spreads and average shifts.

3.1.1. Multipath Scenario with LOS Component and Separable Scattering Function. Consider the case that $S_{\text{diff}}(\tau, \nu)$ is separable, that is,

$$S(\tau, \nu) = \frac{K}{K+1}\delta(\tau)\delta(\nu - \nu_{\text{LOS}}) + \frac{1}{K+1}Q_{\text{diff}}(\tau)P_{\text{diff}}(\nu), \tag{20}$$

where $Q_{\text{diff}}(\tau)$ and $P_{\text{diff}}(\nu)$ denote the PDP and DPP of the scattered components, respectively. Furthermore, assume that $\int_{-\nu_d}^{\nu_d} P_{\text{diff}}(\nu)d\nu = 1$ and $\int_0^{\tau_{\text{diff}}} Q_{\text{diff}}(\tau)d\tau = 1$, where ν_d denotes the maximal Doppler shift and τ_{diff} represents the maximal excess delay. Now, α_i and β_j can be defined as

$$\begin{aligned} \alpha_i &= \int_{-\nu_d}^{\nu_d} P_{\text{diff}}(\nu)\nu^i d\nu, \\ \beta_j &= \int_0^{\tau_{\text{diff}}} Q_{\text{diff}}(\tau)\tau^j d\tau, \end{aligned} \tag{21}$$

respectively. The optimal parameters $c_{0\text{opt}}$ and $c_{1\text{opt}}$ can be expressed as

$$\begin{aligned} c_{0\text{opt}} &= \frac{(K/(K+1))\nu_{\text{LOS}}\beta_2 + (1/(K+1))\alpha_1(\beta_2 - \beta_1^2)}{\beta_2 - (1/(K+1))\beta_1^2}, \\ c_{1\text{opt}} &= \frac{1}{2}\frac{K}{K+1}\frac{\alpha_1\beta_1 - \nu_{\text{LOS}}\beta_1}{\beta_2 - (1/(K+1))\beta_1^2}. \end{aligned} \tag{22}$$

3.1.2. Multipath Scenario with LOS Component and Cluster of Scattered Paths. In the multipath channel with LOS component and cluster of scattered paths, the scattering function takes form

$$S(\tau, \nu) = \frac{K}{K+1}\delta(\tau)\delta(\nu - \nu_{\text{LOS}}) + \frac{1}{K+1}\delta(\tau - \tau_{\text{diff}})P_{\text{diff}}(\nu). \tag{23}$$

For these channels, the optimal parameters $c_{0\text{opt}}$ and $c_{1\text{opt}}$ are

$$c_{0\text{opt}} = \nu_{\text{LOS}},$$
$$c_{1\text{opt}} = \frac{1}{2}\frac{\alpha_1 - \nu_{\text{LOS}}}{\tau_{\text{diff}}}. \tag{24}$$

3.1.3. Multipath Scenario with Two Paths. Often the signal propagates over the two paths, one direct and one reflected. The channel model is further simplified with the scattering function that has nonzero values only in two points $(0, \nu_{\text{LOS}})$ and $(\tau_{\text{diff}}, \nu_{\text{diff}})$, that is,

$$S(\tau,\nu) = \frac{K}{K+1}\delta(\tau)\delta(\nu - \nu_{\text{LOS}}) + \frac{1}{K+1}\delta(\tau - \tau_{\text{diff}})\delta(\nu - \nu_{\text{diff}}). \tag{25}$$

Now, the optimal parameters $c_{0\text{opt}}$ and $c_{1\text{opt}}$ reduce to

$$c_{0\text{opt}} = \nu_{\text{LOS}},$$
$$c_{1\text{opt}} = \frac{1}{2}\frac{\nu_{\text{diff}} - \nu_{\text{LOS}}}{\tau_{\text{diff}}}. \tag{26}$$

In the two-path channel, $m_{20}(c_0, c_1)$, with the optimal parameters, equals 0. Since the interference power depends on $m_{20}(c_0, c_1)$, it is obvious that $P_I = 0$ in the AFT-MC system. It is shown in [3] that the two-path channel represents the worst case for OFDM since the interference equals the upper bound $P_I = (1/3)\nu_{\text{LOS}}^2\pi^2T^2$. On the other hand, two-path channel represents the best case scenario for the AFT-MC system, since the interference is completely removed.

3.2. Synchronization in the AFT-MC Systems. The optimal parameters are also related to the time and frequency synchronization. The time and frequency offsets may occur in case of time delay caused by the multipath and nonideal time synchronization, sampling clock frequency discrepancy, carrier frequency offset (CFO) induced by the Doppler effects or poor oscillator alignments [12]. The problem of time and frequency synchronization has been widely studied in OFDM [13–17]. The effects of time delays can be efficiently evaded by using the GI. If the length of the GI exceeds that of the channel impulse response, there will be no time offset and signal will be perfectly reconstructed. The same approach can be used in the AFT-MC system, since the GI is used in the same manner as in OFDM. Similarly, the frequency offset correction, defined by the parameter c_0, is used in both the AFT-MC and OFDM system. Thus, the offset correction techniques identified for OFDM can be employed in the AFT-MC system. The AFT-MC system, however, also depends on the frequency parameter c_1. The effects of estimation errors can be modeled by using parameter $m_{20}(c_0, c_1)$, which represents the equivalent Doppler spread $\nu_m(c_0, c_1)$

$$\nu_m(c_0,c_1) = \int_{-\nu_d}^{\nu_d}\int_0^{\tau_{\max}} S(\tau,\nu) \times (\nu - c_0 - \varepsilon_0 - 2(c_1+\varepsilon_1)\tau)^2 d\tau\, d\nu, \tag{27}$$

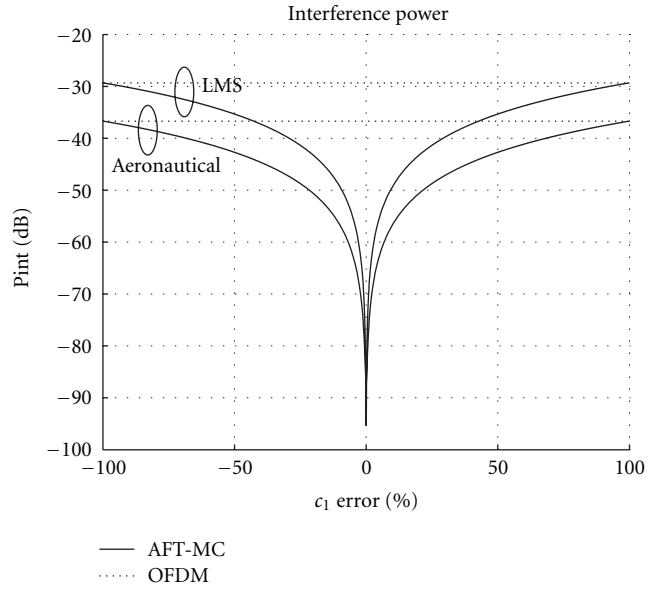

Figure 2: Comparison of the effects of c_1 estimation errors on the interference power in the AFT-MC and OFDM system in aeronautical and LMS channels.

where ε_0 and ε_1 represent errors in estimation of c_0 and c_1, respectively. Since the CFO is the same in the OFDM and AFT-MC system, ε_0 affects the properties of both systems to the similar extent. However, ε_1 affects only the AFT-MC system and it reduces the interference suppression ability of the system.

Inserting $c_0+\varepsilon_0$ and $c_1+\varepsilon_1$ in (27), after some calculation, the difference between Doppler spread in the system with and without estimation errors can be expressed as

$$\Delta\nu_m(c_0,c_1) = \varepsilon_0^2 - 2\varepsilon_0 m_{10}(0,0) - 4\varepsilon_0\varepsilon_1 m_{01}(0,0) + 4\varepsilon_1^2 m_{02}(0,0) + 2\varepsilon_1 m_{11}(0,0). \tag{28}$$

In case that c_1 estimation error is equal to zero, the difference between Doppler spread $\Delta\nu_m(c_0, 0)$ represents an CFO and it depends on m_{10} and ε_0. However, if c_0 estimation error is equal to zero, the difference between Doppler spreads $\Delta\nu_m(c_0, 0)$ represents an offset specific for the AFT-MC system and it depends on m_{01}, m_{02}, m_{11}, and ε_1.

The effects of parameter c_1 estimation errors in aeronautical and LMS channels for $\nu = 20$ m/s are illustrated in Figure 2. The error is expressed as ε_1/c_1. It can be observed that in case of estimation error of 100%, the AFT-MC system has the same properties as the OFDM, whereas for smaller errors the AFT-MC system performs better. Therefore, even if significant estimation error is present, the AFT-MC system is better in interference reduction than the OFDM. This robustness gives a possibility to use the AFT-MC system in the channels where parameters cannot be perfectly obtained. In each presented example, even for 20% error, the interference power in the AFT-MC system in presented examples is still bellow −40 dB.

3.3. Spectral Efficiency Maximization. The multicarrier communication system is expected to be able to efficiently use the available spectrum and combat interference. The symbol is typically preceded by the GI whose duration is longer than the delay spread of the propagation channel. Adding the GI the ISI can be completely eliminated. Although the GI is an elegant solution to cope with the distortions of the multipath channel, it reduces the bandwidth efficiency, which significantly affects the channel utilization. The spectral efficiency can be defined as

$$\eta = \frac{T}{T + T_{\mathrm{CP}}} = \frac{1}{1 + G}, \tag{29}$$

where $G = T_{\mathrm{CP}}/T$ defines the ratio between the symbol and GI durations. This is also a measure of the bit rate reduction required by the GI. Hence, smaller G leads to the higher bit rate. In the OFDM case, to mitigate effects of multipath propagation, the length of the GI has to be chosen as a small fraction of the OFDM symbol length. However, if the OFDM symbol length is long, the ICI caused by the Doppler spreading significantly derogates the system performance. Nevertheless, in the AFT-MC system, the Doppler spreading in time-varying multipath channels is mitigated by the chirp modulation properties, and therefore it is possible to significantly increase the symbol period and maximize η. The AFT-MC system with the GI can reduce interference power, but its spectral efficiency is highly dependable on the symbol period. The optimal symbol period is a trade off between reducing interference to the targeted level and maximizing the spectral efficiency. Inserting (9) into (17), the optimal symbol period can be obtained as

$$T_{\mathrm{opt}} = \sqrt{\frac{3P_I}{m_{20}(c_0, c_1)\pi^2(1 - P_I(K+1))}}. \tag{30}$$

The optimal symbol period, for any predefined P_I, can be directly calculated based on the channel parameters $m_{20}(c_0, c_1)$ and K. The corresponding spectral efficiency η can be easily calculated inserting (30) into (29). Now, for predefined P_I, the corresponding spectral efficiency can be also directly calculated.

The dependence between the spectral efficiency and interference power in aeronautical en-route and LMS channels with the LOS and scattered multipath components is shown in Figure 3. It can be seen that in each scenario, for the spectral efficiency $\eta = 95\%$, the interference power is bellow -40 dB. Therefore, use of the GI interval with the optimal T does not significantly reduce spectral efficiency.

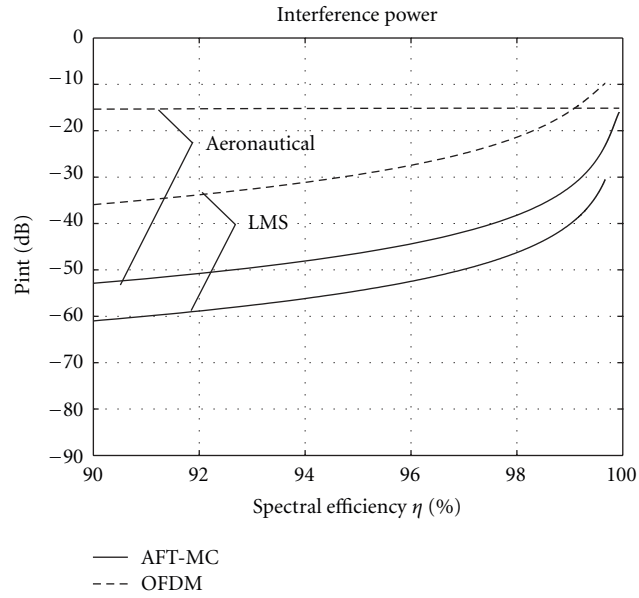

Figure 3: Comparison of the interference power for different spectral efficiency in aeronautical and LMS channels with the LOS and scattered multipath components.

4. Practical Implementation

4.1. AFT-MC in Aeronautical Channels. The aeronautical channel represents a challenging setup for the multicarrier systems. Four different channel scenarios can be defined: en-route, arrival and takeoff, taxi, and parking scenario [18]. These scenarios are characterized by different types of fading, Doppler spreads, and delays. In the parking scenario, only multipath components exist, whereas in all other scenarios there is in addition a strong LOS component. In all scenarios, we take the carrier frequency $f_c = 1.55$ GHz (corresponding to the L band), and the maximum Doppler shift depends on the velocity of the aircraft $\nu_d = \nu_{\max} f_c/c$, where c denotes the speed of light. Other channel parameters are taken from [18]. All interferences powers have been calculated using (16) and (17).

4.1.1. En-Route Scenario. The en-route scenario describes ground-to-air or air-to-air communications when the aircraft is airborne. This multipath channel characterizes a LOS path and cluster of scattered paths. Typical maximal speeds are $\nu_{\max} = 440$ m/s for ground-air links and $\nu_{\max} = 620$ m/s for air-air links. In this scenario, the scattered components are not uniformly distributed in the interval $[0, 2\pi)$ leading to the asymmetrical DPP. Actually, the beamwidth of the scattered components is reported to be $\Delta\varphi_B = 3.5^\circ$ [18]. Maximal excess delay equals $\tau_{\mathrm{diff}} = 66\,\mu$s, and Rician factor is $K = 15$ dB. In this case, $S(\tau, \nu)$ takes form (23). The DPP can be modeled by the restricted Jakes model [19]

$$P_{\mathrm{diff}}(\nu) = \psi \frac{1}{\nu_d \sqrt{1 - (\nu/\nu_d)^2}}, \quad \nu_1 \le \nu \le \nu_2, \tag{31}$$

and $\psi = 1/(\arcsin(\nu_2/\nu_d) - \arcsin(\nu_1/\nu_d))$ denotes a factor introduced to normalize the DPP.

Consider the worst case when the LOS component comes directly to the front of the aircraft and scattered components come from behind. Now, $\nu_1 = -\nu_d$ and $\nu_2 = -\nu_d(1 - \Delta\varphi_B/\pi)$, where $\Delta\varphi_B$ represents the beamwidth of the scattered components symmetrically distributed around $\varphi = \pi$.

For this model, parameters $m_{0j}(0,0)$ for $j \in N$ can be calculated as

$$m_{0j}(0,0) = \frac{1}{K+1}\tau_{\text{diff}}^{j}. \tag{32}$$

Moments $m_{i0}(0,0)$ can be directly calculated from (13). The first two moments can be obtained as

$$m_{10}(0,0) = \frac{K}{K+1}\nu_{\text{LOS}} + \frac{1}{K+1}\psi\left(\sqrt{\nu_d^2-\nu_1^2} - \sqrt{\nu_d^2-\nu_2^2}\right), \tag{33}$$

$$m_{20}(0,0) = \frac{K}{K+1}\nu_{\text{LOS}}^2 + \frac{1}{K+1}\frac{\psi}{2} \times\left(\nu_1\sqrt{\nu_d^2-\nu_1^2} - \nu_2\sqrt{\nu_d^2-\nu_2^2}\right) + \frac{1}{2}\frac{\nu_d^2}{K+1}. \tag{34}$$

Now, parameters $m_{ij}(0,0)$ for $i > 0$ and $j > 0$ can be recursively calculated as

$$m_{ij}(0,0) = m_{0j}(0,0)(K+1)\left(m_{i0}(0,0) - \frac{K}{K+1}\nu_{\text{LOS}}^{i}\right). \tag{35}$$

Figure 4 illustrates the comparison of the interference power obtained for the OFDM and AFT-MC system with and without the GI in the en-route scenario for different T and aircraft velocity $v = 400$ m/s. From Figure 4 it can be observed that even without the GI, the AFT-MC system is significantly better in suppressing the interference in comparison to the OFDM with the GI. In the AFT-MC system, the ICI is significantly reduced by the properties of the system and larger T can be implemented in order to combat ISI. Thus, in the en-route scenario, AFT-MC significantly suppresses the total interference power. In case that the GI is used, even better interference reduction can be achieved with slightly lower spectral efficiency. It can be observed that the interference power for the AFT-MC system with the GI even for the extremely high aircraft velocity of $v = 400$ m/s can be below -40 dB. Note that even without the GI interference power below -28 dB can be achieved.

4.1.2. Arrival and Takeoff Scenario. The arrival and takeoff scenario models communications between ground and aircraft when the aircraft takeoffs or is about to land. It is assumed that the LOS and scattered components arrive directly in front of the aircraft and the beamwidth of the scattered components from the obstacles in the airport is 180°. The maximal speed of the aircraft is 150 m/s, and the Rician factor $K = 15$ dB. In this channel, $S(\tau,\nu)$ takes form (20). The PDP can be modeled as an exponential function similarly to the rural nonhilly COST 207 model [10]

$$Q_{\text{diff}}(\tau) = \begin{cases} c_n e^{-t/\tau_s} & \text{if } 0 \le \tau < \tau_{\text{diff}}, \\ 0, & \text{elsewhere,} \end{cases} \tag{36}$$

where τ_{diff} denotes the maximal excess delay, τ_s characterizes the slope of the function, and

$$c_n = \frac{1}{\tau_s(1 - e^{-\tau_{\text{diff}}/\tau_s})} \tag{37}$$

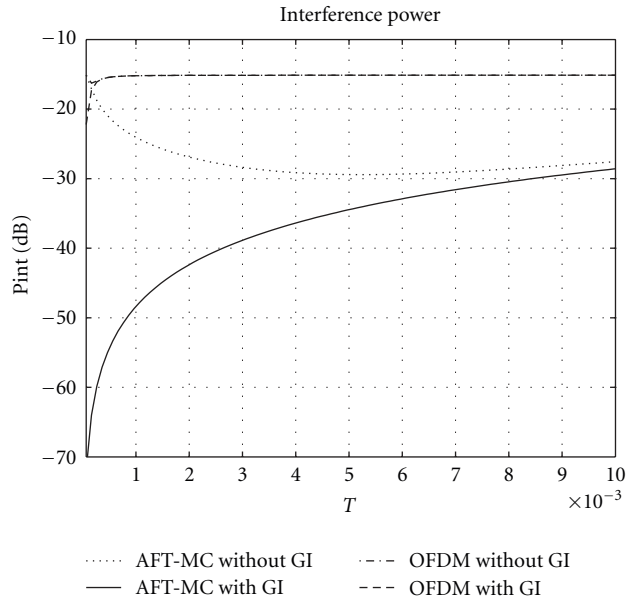

Figure 4: Comparison of the interference power in the en-route scenario for the AFT-MC and OFDM system.

represents the normalization factor. For the rural nonhilly model, $\tau_{\text{diff}} = 0.7\,\mu$s and $\tau_s = 1/9.2\,\mu$s.

The DPP can be modeled by the restricted Jakes model (31), with $\nu_1 = 0$ and $\nu_2 = \nu_d$. Parameters $m_{10}(0,0)$ and $m_{20}(0,0)$ can be obtained by inserting ν_1 and ν_2 into (33) and (34), respectively.

Parameters $m_{0j}(0,0)$ for $j \in N$ can be calculated recursively as

$$m_{0j}(0,0) = m_{0j-1}(0,0)j\tau_s - \frac{1}{K+1}c_n\tau_s e^{-\tau_{\text{diff}}/\tau_s}\tau_{\text{diff}}^{j}, \tag{38}$$

where $m_{01}(0,0) = (1/(K+1))c_n\tau_s(\tau_s - e^{-\tau_{\text{diff}}/\tau_s}(\tau_{\text{diff}} + \tau_s))$. Moments $m_{ij}(0,0)$ can be calculated from (35).

Figure 5 shows the comparison of the interference power in the OFDM and AFT-MC system with and without the GI in the arrival and takeoff scenario for different T and aircraft velocity $v = 100$ m/s. The AFT-MC system still outperforms the OFDM, since the beamwidth of the multipath component is 180°. Similarly to the previous case, introduction of the GI efficiently combats the interference for shorter symbol periods.

4.1.3. Taxi Scenario. The taxi scenario is a model for communications when the aircraft is on the ground and approaching or moving away from the terminal. The LOS path comes from the front, but not directly, resulting in smaller Doppler shifts, in this example $\nu_{\text{LOS}} = 0.7\nu_d$. The maximal speed is 15 m/s, the Rician factor $K = 6.9$ dB, and the reflected paths come uniformly, resulting in the classical Jakes DPP (31), with $\nu_1 = -\nu_d$ and $\nu_2 = \nu_d$. Inserting ν_1 and ν_2 into (33) and (34) parameters $m_{10}(0,0)$ and $m_{20}(0,0)$ can be, respectively, calculated.

The PDP can be modeled similarly to the rural (nonhilly) COST 207 model by the exponential function (36) with the

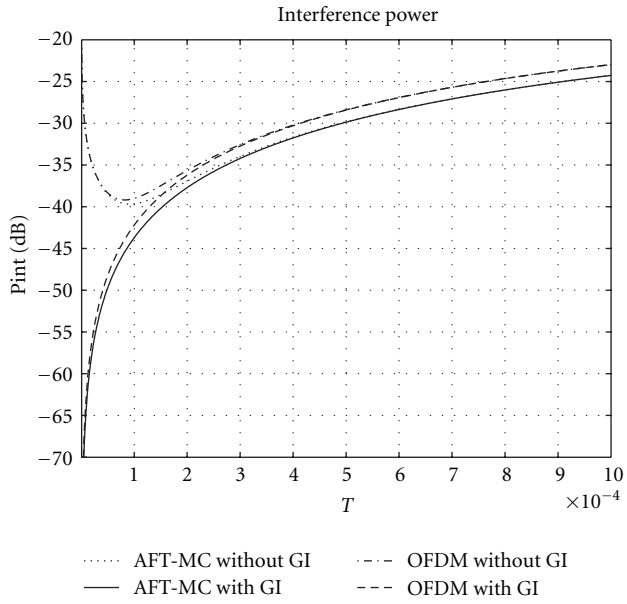

Figure 5: Comparison of the interference power in the arrival and takeoff scenario for the AFT-MC and OFDM system.

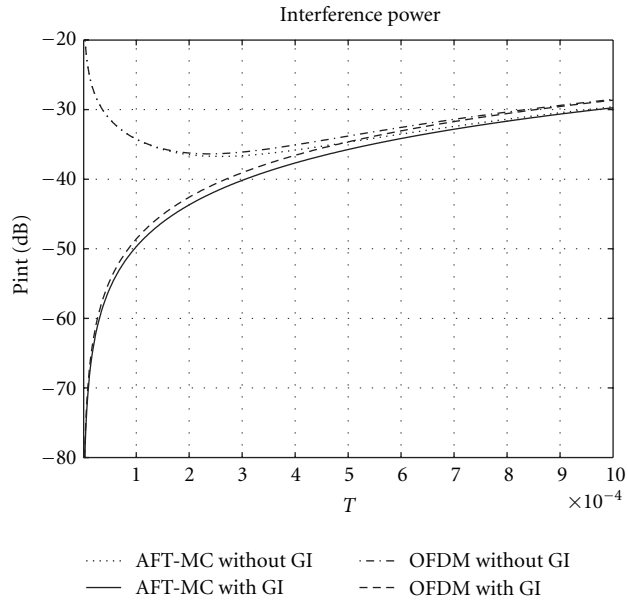

Figure 6: Comparison of the interference power in the taxi scenario for the AFT-MC and OFDM system.

maximal excess delay of $\tau_{\text{diff}} = 0.7\,\mu$s and $\tau_s = 1/9.2\,\mu$s. Moments $m_{ij}(0,0)$ can be calculated from (35).

The comparison of the interference power in the OFDM and AFT-MC systems with and without the GI, in the taxi scenario for different T and aircraft velocity $v = 10$ m/s is shown in Figure 6. Since the PDP has exponential profile and the beamwidth of the multipath component is 360°, interference characteristics of the OFDM and AFT-MC system are closer comparing to the previous example. However, it can been observed that the interference power in the AFT-MC system is still lower than in the OFDM, since the AFT-MC system exploits the existence of LOS component.

4.1.4. Parking Scenario. The parking scenario models the arrival of the aircraft to the terminal or parking. The LOS path is blocked, resulting in Rayleigh fading. The maximal speed of the aircraft is 5.5 m/s, and the DPP can be modeled as the classical Jakes profile (31) with $\nu_1 = -\nu_d$ and $\nu_2 = \nu_d$. The parking scenario is similar to the typical urban COST 207 model, with the exponential PDP (36), $\tau_{\text{diff}} = 7\,\mu$s, and slope time $\tau_s = 1\,\mu$s [10].

Figure 7 shows the comparison of the interference power in the OFDM and AFT-MC system with and without the GI in the parking scenario for different T and aircraft velocity $v = 2.5$ m/s. Since there is no LOS and DPP is symmetrical, the AFT-MC system reduces to the ordinary OFDM ($c_0 = 0$). Thus, there is no difference in characteristics between the MC-AFT and OFDM.

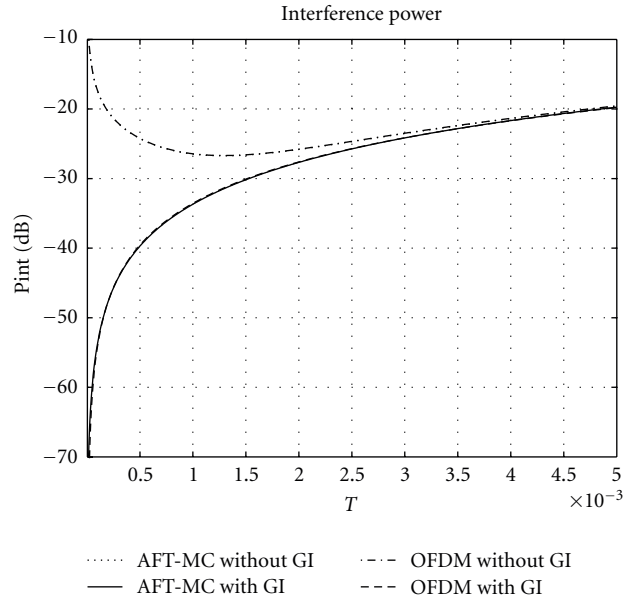

Figure 7: Comparison of the interference power in the parking scenario for the AFT-MC and OFDM system.

4.2. AFT-MC in Land-Mobile Satellite Channels. The LMS channel represents another example of environment with strong LOS component and scattered multipath components. We will discuss different cases of Land-Mobile Low Earth Orbit (LEO) satellite channels. In the following examples, it is assumed that carrier frequency $f_c = 1.55$ GHz, Rician factor $K = 7$ dB, and the maximal velocity is up to $v_{\max} = 50$ m/s. In each example, the AFT-MC system is compared to the OFDM with the offset correction. The interference powers are calculated using (16) and (17).

Consider the LMS channel, where a mobile terminal uses a narrow-beam antenna (e.g., digital beamforming (DBF) antenna) to track and communicate with satellite. Note that in case where a directive antenna is employed at the user terminal, the classical Jakes model is no longer applicable [20].

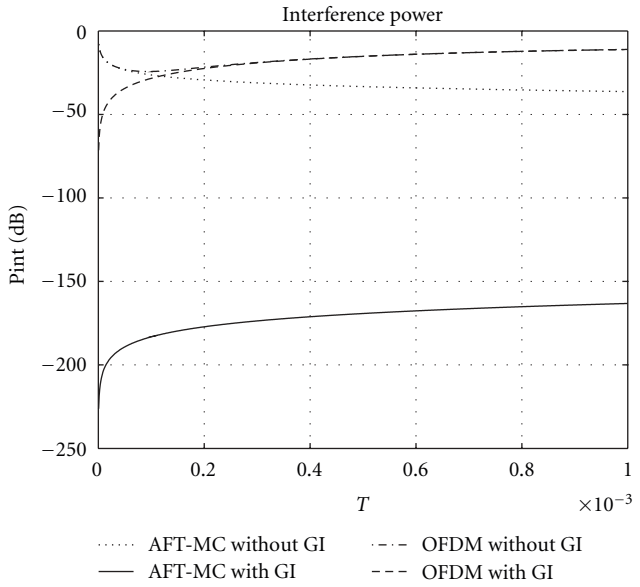

Figure 8: Comparison of the AFT-MC and OFDM interference power in the two-path LMS channel.

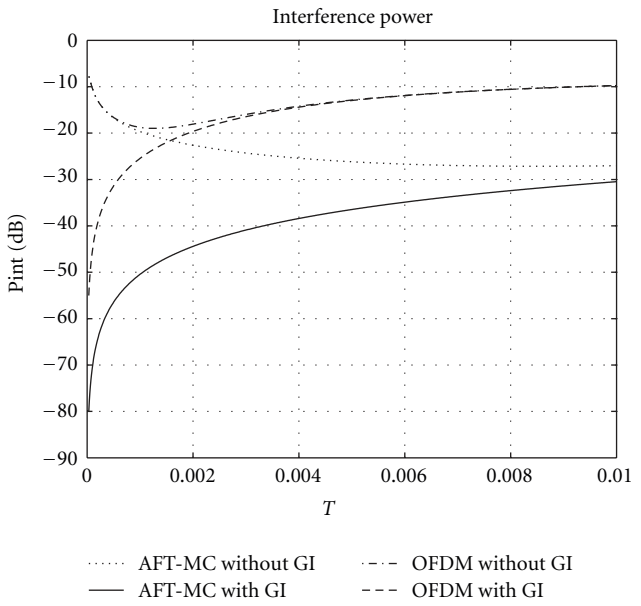

Figure 9: Comparison of the AFT-MC and OFDM interference power in the LMS channel with LOS component and cluster of scattered paths.

4.2.1. Two-Path. Let us first consider the two-path channel model, with $\nu_{\text{diff}} = -\nu_d$, $\nu_{\text{LOS}} = \nu_d$, and $\tau_{\text{diff}} = 0.7\,\mu$s. The channel is characterized by the scattering function given in (25), whereas the optimal parameters can be calculated from (26). Figure 8 compares the interference power for the OFDM and AFT-MC systems. It is obvious that the AFT-MC system completely eliminates interference, whereas interference in OFDM has significant value. Thus, in the two-path LMS channels, the AFT-MC system is the optimal one.

4.2.2. LOS and Scattered Multipath Components. Consider the channel model with LOS and scattered multipath components that arrives at the receiver at $\tau_{\text{diff}} = 33\,\mu$s. The channel is characterized by the scattering function given in (23), whereas DPP can be modeled by the asymmetrical restricted Jakes model (31). Note that this case DPP is similar to the en-route scenario in aeronautical channels. However, in this example, the arrival angles of the multipath components are uniformly distributed, but the antenna is narrow-beam. Let us assume that the angle between the direction of travel and the antenna bearing angle is $\eta = 15^\circ$, the elevation angle of the satellite transmitter relative to the mobile receiver is $\xi = 45^\circ$, and the antenna beamwidth is $\beta = 12^\circ$. Here, $\nu_1 = \nu_d \cos(\eta + \beta/2)$, $\nu_2 = \nu_d \cos(\eta - \beta/2)$, and $\nu_{\text{LOS}} = \nu_d \cos(\xi)\cos(\eta)$ [21].

Figure 9 compares the interference power for the OFDM and AFT-MC systems. It can be observed that the AFT-MC system clearly outperforms OFDM. Thus, the implementation of the AFT-MC system in the LMS channels with LOS path and scattered multipath components leads to the significant reduction of interference.

4.2.3. LOS and Exponential Multipath Components. This channel is described by the scattering functions given in (20). Assume that the mobile terminal is out of urban areas, and PDP can be modeled as an exponential function similarly to the rural nonhilly COST 207 model (36). The DPP is asymmetrical and it can be modeled by the restricted Jakes model (31). Figure 10 shows the comparison of the interference power in the OFDM and AFT-MC systems in the LMS scenario with narrow-beam antenna. It can be observed that the AFT-MC system outperforms the OFDM when the narrow-beam antenna is used.

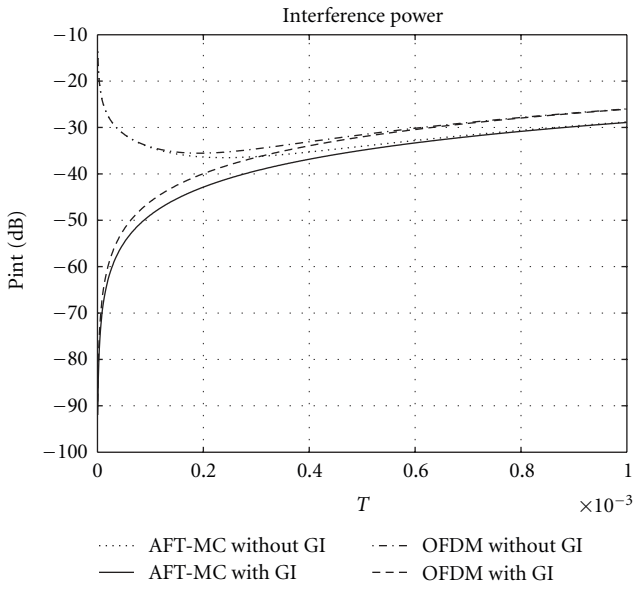

Figure 10: Comparison of the AFT-MC and OFDM interference power in the LMS channel with LOS component and COST 207 multipath model.

5. Conclusion

In this paper, we present performance analysis of the AFT-MC systems in doubly dispersive channels with focus on aeronautical and LMS channels. The upper and lower bounds on interference power are given, followed by an approximation of the interference power, based on the modified upper bound, that significantly simplify calculation. The optimal parameters are obtained in a closed form, and practical examples for their calculation are given.

Since the AFT-MC system can be considered as a generalization of the OFDM, it is applicable in all channels where the OFDM is used with, at least, the same performance. Additional improvements, due to resilience to the interference in time-varying wireless channels with significant Doppler spread and LOS component, offer new possibilities in designing multicarrier systems for aeronautical and LMS communications. It has been shown that the spectral efficiency higher than 95% can be achieved, with an acceptable level of interference.

References

[1] T. Erseghe, N. Laurenti, and V. Cellini, "A multicarrier architecture based upon the affine fourier transform," *IEEE Transactions on Communications*, vol. 53, no. 5, pp. 853–862, 2005.

[2] D. Stojanović, I. Djurović, and B. R. Vojcic, "Interference analysis of multicarrier systems based on affine fourier transform," *IEEE Transactions on Wireless Communications*, vol. 8, no. 6, pp. 2877–2880, 2009.

[3] Y. Li and L. J. Cimini, "Bounds on the interchannel interference of OFDM in time-varying impairments," *IEEE Transactions on Communications*, vol. 49, no. 3, pp. 401–404, 2001.

[4] T. Gilbert, J. Jin, J. Berger, and S. Henriksen, "Future aeronautical communication infrastructure technology investigation," Tech. Rep. NASA/CR-2008-215144, NASA, Los Angeles, Calif, USA, April 2008.

[5] W. W Wu, "Satellite communications," *Proceedings of the IEEE*, vol. 85, no. 6, pp. 998–1010, 1997.

[6] J. V. Evans, "Satellite systems for personal communications," *Proceedings of the IEEE*, vol. 86, no. 7, pp. 1325–1340, 1998.

[7] P. A. Bello, "Characterization of randomly time-variant linear channels," *IEEE Transactions on Communications Systems*, vol. 11, no. 4, pp. 360–393, 1963.

[8] M. Abramowitz and I. A. Stegun, *Handbook of Mathematical Functions*, Dover, New York, NY, USA, 1964.

[9] J. G. Proakis, *Digital Communications*, McGraw-Hill, New York, NY, USA, 4th edition, 2000.

[10] M. Falli, Ed., "Digital land mobile radio communications-COST 207: final report," Tech. Rep., Commission of European Communities, Luxembourg, Germany, 1989.

[11] S. Barbarossa and R. Torti, "Chirped-OFDM for transmissions over time-varying channels with linear delay/Doppler spreading," in *Proceedings of the IEEE Interntional Conference on Acoustics, Speech, and Signal Processing (ICASSP '01)*, pp. 2377–2380, Salt Lake City, Utah, USA, May 2001.

[12] D. Huang and K. B. Letaief, "An interference-cancellation scheme for carrier frequency offsets correction in OFDMA systems," *IEEE Transactions on Communications*, vol. 53, no. 7, pp. 1155–1165, 2005.

[13] P. H. Moose, "Technique for orthogonal frequency division multiplexing frequency offset correction," *IEEE Transactions on Communications*, vol. 42, no. 10, pp. 2908–2914, 1994.

[14] T. Pollet and M. Moeneclaey, "Synchronizability of OFDM signals," in *Proceedings of the IEEE Global Telecommunications Conference (Globecom '95)*, pp. 2054–2058, Singapore, November 1995.

[15] J. J. van de Beek, M. Sandell, and P. O. Börjesson, "ML estimation of time and frequency offset in OFDM systems," *IEEE Transactions on Signal Processing*, vol. 45, no. 7, pp. 1800–1805, 1997.

[16] T. M. Schmidl and D. C. Cox, "Robust frequency and timing synchronization for OFDM," *IEEE Transactions on Communications*, vol. 45, no. 12, pp. 1613–1621, 1997.

[17] B. Yang, K. B. Letaief, R. S. Cheng, and Z. Cao, "Timing recovery for OFDM transmission," *IEEE Journal on Selected Areas in Communications*, vol. 18, no. 11, pp. 2278–2291, 2000.

[18] E. Haas, "Aeronautical channel modeling," *IEEE Transactions on Vehicular Technology*, vol. 51, no. 2, pp. 254–264, 2002.

[19] M. Paetzold, *Mobile Fading Channels*, John Wiley & Sons, New York, NY, USA, 2002.

[20] C. Kasparis, P. King, and B. G. Evans, "Doppler spectrum of the multipath fading channel in mobile satellite systems with directional terminal antennas," *IET Communications*, vol. 1, no. 6, pp. 1089–1094, 2007.

[21] M. Rice and E. Perrins, "A simple figure of merit for evaluating interleaver depth for the land-mobile satellite channel," *IEEE Transactions on Communications*, vol. 49, no. 8, pp. 1343–1353, 2001.